

REPORT DOCUMENTATION PAGE			Form Approved OMB NO. 0704-0188	
<p>The public reporting burden for this collection of information is estimated to average 1 hour per response, including the time for reviewing instructions, searching existing data sources, gathering and maintaining the data needed, and completing and reviewing the collection of information. Send comments regarding this burden estimate or any other aspect of this collection of information, including suggestions for reducing this burden, to Washington Headquarters Services, Directorate for Information Operations and Reports, 1215 Jefferson Davis Highway, Suite 1204, Arlington VA, 22202-4302. Respondents should be aware that notwithstanding any other provision of law, no person shall be subject to any penalty for failing to comply with a collection of information if it does not display a currently valid OMB control number.</p> <p>PLEASE DO NOT RETURN YOUR FORM TO THE ABOVE ADDRESS.</p>				
1. REPORT DATE (DD-MM-YYYY)		2. REPORT TYPE		3. DATES COVERED (From - To)
		New Reprint		-
4. TITLE AND SUBTITLE			5a. CONTRACT NUMBER	
Structure and magnetism of nanocrystalline and epitaxial (Mn,Zn,Fe)3O4 thin films			W911NF-08-1-0317	
			5b. GRANT NUMBER	
			5c. PROGRAM ELEMENT NUMBER	
			611103	
6. AUTHORS			5d. PROJECT NUMBER	
F. J. Wong, A. J. Grutter, J. M. Iwata-Harms, V. V. Mehta, U. S. Alaan, E. Arenholz, Y. Suzuki				
			5e. TASK NUMBER	
			5f. WORK UNIT NUMBER	
7. PERFORMING ORGANIZATION NAMES AND ADDRESSES			8. PERFORMING ORGANIZATION REPORT NUMBER	
University of Iowa @ Iowa City Office of Sponsored Programs The University of Iowa Iowa City, IA 52242 -				
9. SPONSORING/MONITORING AGENCY NAME(S) AND ADDRESS(ES)			10. SPONSOR/MONITOR'S ACRONYM(S) ARO	
U.S. Army Research Office P.O. Box 12211 Research Triangle Park, NC 27709-2211			11. SPONSOR/MONITOR'S REPORT NUMBER(S)	
			54223-MS-MUR.37	
12. DISTRIBUTION AVAILABILITY STATEMENT				
Approved for public release; distribution is unlimited.				
13. SUPPLEMENTARY NOTES				
The views, opinions and/or findings contained in this report are those of the author(s) and should not be construed as an official Department of the Army position, policy or decision, unless so designated by other documentation.				
14. ABSTRACT				
Nanocrystalline (NC) textured Mn _{0.5} Zn _{0.6} Fe _{1.9} O ₄ (MZFO) films, grown at room temperature on both isostructural and non-isostructural substrates, show magnetization values significantly suppressed from epitaxial MZFO films. X-ray absorption spectroscopy and x-ray magnetic circular dichroism measurements indicate larger ratios of Fe ³⁺ to Fe ²⁺ ions on the tetrahedral sites in the NC films compared to the epitaxial films. The magnetization loops of the NC films are shifted by 200°/400 Oe				
15. SUBJECT TERMS				
structure, magnetism, nanocrystalline, films				
16. SECURITY CLASSIFICATION OF:			17. LIMITATION OF ABSTRACT	15. NUMBER OF PAGES
a. REPORT	b. ABSTRACT	c. THIS PAGE	UU	19a. NAME OF RESPONSIBLE PERSON
UU	UU	UU		Michael Flatte
				19b. TELEPHONE NUMBER
				319-335-0201

Report Title

Structure and magnetism of nanocrystalline and epitaxial $(\text{Mn,Zn,Fe})_3\text{O}_4$ thin films

ABSTRACT

Nanocrystalline (NC) textured $\text{Mn}_{0.5}\text{Zn}_{0.6}\text{Fe}_{1.9}\text{O}_4$ (MZFO) films, grown at room temperature on both isostructural and non-isostructural substrates, show magnetization values significantly suppressed from epitaxial MZFO films. X-ray absorption spectroscopy and x-ray magnetic circular dichroism measurements indicate larger ratios of Fe^{3+} to Fe^{2+} ions on the tetrahedral sites in the NC films compared to the epitaxial films. The magnetization loops of the NC films are shifted by 200-400 Oe at low temperatures. No such effect is observed in the epitaxial films. We hypothesize that the presence of a more structurally disordered, possibly magnetically frustrated, matrix exchange biases the crystalline regions

REPORT DOCUMENTATION PAGE (SF298)
(Continuation Sheet)

Continuation for Block 13

ARO Report Number 54223.37-MS-MUR
Structure and magnetism of nanocrystalline and ...

Block 13: Supplementary Note

© 2012 . Published in Journal of Applied Physics, Vol. Ed. 0 111, (7) (2012), (, (7). DoD Components reserve a royalty-free, nonexclusive and irrevocable right to reproduce, publish, or otherwise use the work for Federal purposes, and to authorize others to do so (DODGARS §32.36). The views, opinions and/or findings contained in this report are those of the author(s) and should not be construed as an official Department of the Army position, policy or decision, unless so designated by other documentation.

Approved for public release; distribution is unlimited.

Structure and magnetism of nanocrystalline and epitaxial (Mn,Zn,Fe)₃O₄ thin films

U. S. Alaan,^{1,a)} F. J. Wong,¹ A. J. Grutter,^{1,2} J. M. Iwata-Harms,¹ V. V. Mehta,^{1,2}
E. Arenholz,³ and Y. Suzuki^{1,2}

¹Department of Materials Science and Engineering, UC Berkeley, Berkeley, California 94720, USA

²Materials Sciences Division, Lawrence Berkeley National Laboratory, Berkeley, California 94720, USA

³Advanced Light Source, Lawrence Berkeley National Laboratory, Berkeley, California 94720, USA

(Presented 31 October 2011; received 24 September 2011; accepted 14 November 2011; published online 21 February 2012)

Nanocrystalline (NC) textured Mn_{0.5}Zn_{0.6}Fe_{1.9}O₄ (MZFO) films, grown at room temperature on both isostructural and non-isostructural substrates, show magnetization values significantly suppressed from epitaxial MZFO films. X-ray absorption spectroscopy and x-ray magnetic circular dichroism measurements indicate larger ratios of Fe³⁺ to Fe²⁺ ions on the tetrahedral sites in the NC films compared to the epitaxial films. The magnetization loops of the NC films are shifted by 200–400 Oe at low temperatures. No such effect is observed in the epitaxial films. We hypothesize that the presence of a more structurally disordered, possibly magnetically frustrated, matrix exchange biases the crystalline regions. © 2012 American Institute of Physics. [doi:10.1063/1.3676619]

Thin films and nanoparticles of spinel structure oxides exhibit a range of functional properties through variation of cation species, lattice distortions, and crystallite size.¹ By varying one or more of these factors, we can modify the magnetic, electrical, or optical properties of these materials. Furthermore, transition-metal spinel oxides have cations that can manifest themselves in different valence states, making them particularly sensitive to optical excitation. In particular, photomagnetism has been observed in a few spinel structure materials,^{2,3} including doped spinel structure ferrites and chalcogenide spinels.^{4–6} In these materials, photomagnetism is understood to arise from light induced electronic transitions that give rise to electron redistribution among cations. Initially, effects had been observed primarily at low temperatures. More recently, nanocrystalline (NC) spinel structure ferrite films have been identified to exhibit photomagnetic effects at room temperature.^{7,8} Because optical sensitivity of spinel ferrites can be greatly affected by cation and microstructural disorder, a detailed study of the correlation between the structural and magnetic properties of these NC films is imperative for understanding the origin of the photomagnetic functionality.

In this paper, we present a study correlating the structure of NC and epitaxial (Mn,Zn,Fe)₃O₄ (MZFO) spinel thin films with their magnetic properties. X-ray diffraction (XRD) studies indicate that room temperature growths of MZFO on both isostructural and non-isostructural substrates give rise to textured NC films while high temperature growths on isostructural substrates yield epitaxial films. At low temperatures, NC films exhibit a shift in the magnetic hysteresis, which is not seen in the epitaxial films. The existence of a disordered, magnetically frustrated matrix may explain reduced magnetization in the NC films and the

apparent exchange bias. X-ray absorption spectroscopy (XAS) and x-ray magnetic circular dichroism (XMCD) show that NC films have more tetrahedrally coordinated Fe³⁺ relative to octahedrally coordinated Fe²⁺ and Fe³⁺.

All thin film samples were prepared using pulsed laser deposition (PLD) (KrF laser with fluence of ~ 1.2 J/cm²) with a target of composition Mn_{0.5}Zn_{0.6}Fe_{1.9}O₄. In this study, MZFO thin films were grown on (001) Si and (110) MgAl₂O₄ (MAO) substrates at room temperature in a background pressure of approximately 9×10^{-7} Torr and with a laser repetition rate of 10 Hz. For comparison, epitaxial MZFO films were grown on (110) MAO at 410 °C in 18.2 mTorr of a 99%N₂/1%O₂ mixture with a laser repetition rate of 5 Hz. Film thickness ranged from 180 nm for samples grown in a 99%N₂/1%O₂ environment to 280 nm for those deposited in vacuum, as measured by Rutherford backscattering spectrometry (RBS).

Structural characterization indicates that regardless of substrate choice and deposition conditions, all MZFO films in this study are textured along the out-of-plane [110] direction. The normalized θ - 2θ spectra in Figure 1 demonstrate that MZFO films grown on (001) Si and (110) MAO show only substrate peaks and the $hh0$ MZFO reflections. The films deposited in 18.2 mTorr of 99% N₂/1% O₂ were found to be epitaxial through ϕ scans, thus confirming two-fold symmetry about the (110) plane for both the film and substrate. As expected, these epitaxial films on (110) MAO have the sharpest diffraction peaks and smallest FWHM values, with $\Delta\omega = 0.7^\circ$ in the out-of-plane reflection. Room temperature grown samples on MAO have broader film peaks with typical FWHM values of about $\Delta\omega = 1.5^\circ$. The θ - 2θ spectra show that the room temperature deposited films have larger lattice parameters (8.58 Å) compared to their epitaxial counterparts (8.50 Å) and the PLD target's lattice constant. The larger lattice parameter may be related to structural disorder associated with low temperature thin film

^{a)}Author to whom correspondence should be addressed. Electronic mail: usalaan@gmail.com.

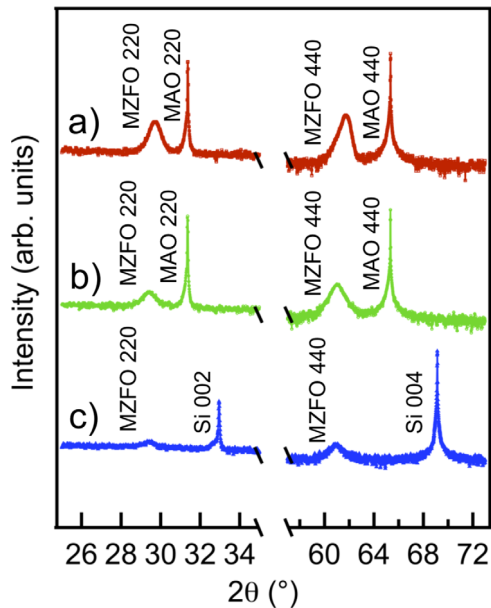


FIG. 1. (Color online) XRD θ - 2θ scans for (a) an epitaxial film on (110) MAO, (b) a NC film on (110) MAO, and (c) a NC film on (001) Si, all showing only the (220) and (440) reflections for MZFO.

growth. RBS revealed that the films had lower relative concentrations of zinc and oxygen compared to the PLD target stoichiometry of $\text{Mn}_{0.5}\text{Zn}_{0.6}\text{Fe}_{1.9}\text{O}_4$, due to the volatility of zinc. It is difficult to use RBS to accurately estimate the atomic concentrations in MZFO due to the similar cation atomic masses and standard complications with characterizing oxygen. Nonetheless, a rough simulation showed that while the Mn:Zn ratio (normalized to Fe) for the target is 0.81, the Mn:Zn ratios for a room temperature deposited film on (001) Si, a room temperature deposited film on (110) MAO and the high temperature deposited film on (110) MAO are 1.5, 1.1, and 1.6, respectively.

While strong preferred orientation in MZFO films deposited at room temperature on isostructural substrates is somewhat surprising, perhaps even more unexpected is the emergence of highly textured films grown at room temperature on (001) Si, a non-isostructural substrate with a large lattice mismatch. Films on (001) Si exhibit both the broadest diffraction peaks ($\Delta\omega = 4.5^\circ$) and the largest lattice parameters ($\sim 8.60 \text{ \AA}$). Since $\Delta\omega$ scans provide a measure of the in-plane crystalline quality, it is clear that higher temperature growth and isostructural substrate choice are essential for high crystallinity; however, our results show that low temperature growth on an isostructural substrate can indeed stabilize some degree of registry between the substrate and overlying film. The texture, observed even in films grown on non-isostructural (001) Si substrates at low temperatures, suggests that the energetic plume in PLD plays a significant role in microstructural ordering. If we assume that XRD peak broadening is due exclusively to size effects and not strain, then we can use Scherrer analysis to estimate a particle size^{9,10} of about 10 nm. The FWHMs for both θ - 2θ and ω scans follow the same trend, suggesting that defects, as well as crystallite size, contribute to peak broadening. The films on silicon have rocking curve FWHMs that are approximately six

times broader than those of the epitaxial samples on MAO and over three times broader than those of the NC films on MAO. These results indicate that despite room temperature deposition conditions, the substrate still imposes a significant degree of crystallographic ordering that is sustained by the system.

Variations in growth conditions and substrate choice for MZFO films can give rise to appreciable differences in the magnetization loops as measured by SQUID magnetometry (Figure 2). Epitaxial samples on (110) MAO appear to saturate near 680 emu/cm^3 at 10 K. By comparison, NC films reach magnetization values of around 160 emu/cm^3 at 5 T but do not appear to saturate. At low temperatures, NC films also reveal a shift in the hysteresis loops, while no such behavior is observed at any temperature in the epitaxial samples. We define the coercive field H_c to be the average of the absolute values of the two fields at which the magnetization is zero. H_c is around 30 Oe for all films measured at 300 K. After field cooling in $\pm 5 \text{ T}$ to 10 K, the NC samples on both Si and MAO have H_c values of about 1100 Oe and 1600 Oe, respectively. The epitaxial films exhibit considerably smaller H_c values of approximately 350 Oe at 10 K. Larger coercive fields in the NC samples are expected since defective regions most likely pin domain walls.¹¹

In order to understand further the differences in the magnetic properties for the NC and epitaxial films, we examined more closely the magnetization loops at low temperatures. Using conventional notation from classic antiferromagnetic-ferromagnetic cases of exchange bias, we define the exchange field H_{ex} to be the shift of the loops from the origin by taking the average value of the fields associated with the two zero magnetization crossings, as shown in the inset of Figure 2. While exchange bias is commonly known to occur between an antiferromagnet and a ferromagnet, we report on the rare case of exchange bias in a single-material system. Venzke *et al.* have also shown that such an effect can occur between ferromagnetic and adjacent glassy magnetic regions in the same material.¹² Our hysteresis loops at 10 K of the NC samples appear to be shifted to negative and positive fields for +5 T and -5 T field cooling, respectively. H_{ex} is about 200 Oe for the NC MZFO films on (001) Si and 380 Oe for the NC

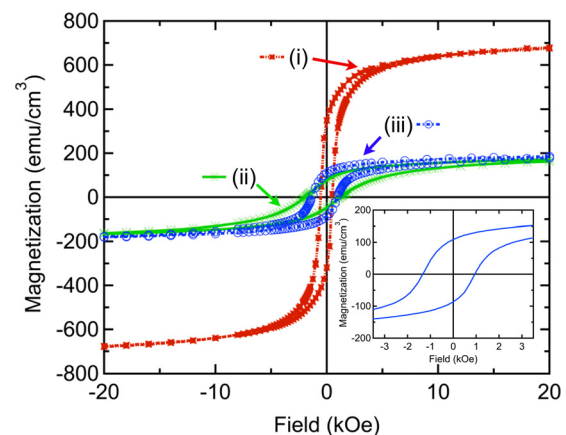


FIG. 2. (Color online) SQUID magnetization curves at 10 K, field-cooled in 5 T of (i) an epitaxial MZFO film on (110) MAO, (ii) a NC film on (110) MAO and (iii) a NC film on (001) Si. Inset shows the exchange biased nanocrystalline film on (001) Si.

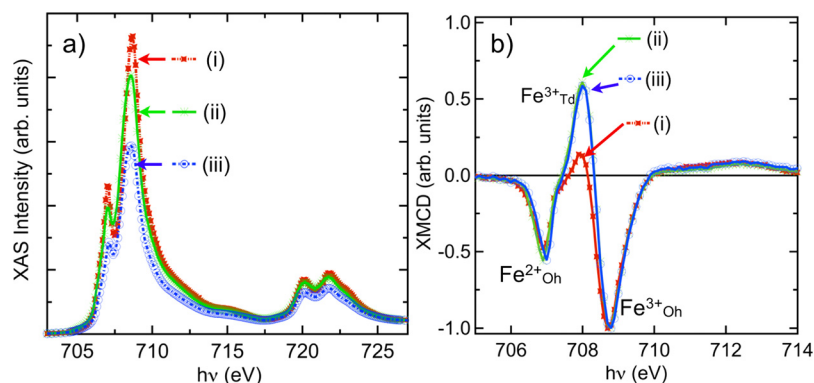


FIG. 3. (Color online) (a) XAS and (b) XMCD of iron ions at 30° incidence and 300 K in (i) an epitaxial MZFO film on (110) MAO, (ii) a NC film on (110) MAO and (iii) a NC film on (001) Si. The site occupancies corresponding to the peaks in XMCD are labeled, with “Oh” and “Td” denoting octahedral and tetrahedral sites, respectively.

MZFO films on MAO. The slightly larger exchange bias field values for the NC samples on MAO is a manifestation of stronger coupling between defective, magnetically frustrated regions with more crystalline ferrimagnetic regions.^{11,12} XRD indicated that the epitaxial films are less defective. Consequently, we observe that under the same ± 5 T field-cooled conditions, the epitaxial film exhibits little to no shift away from the origin at 10 K. Exchange biasing vanished in hysteresis loops for all NC and epitaxial samples at room temperature; this observation indicates that in NC films the frustrated regions no longer effectively bias the ferromagnetic regions due to thermal considerations at temperatures as high as 300 K. Thus, the existence of magnetically frustrated regions allows us to account for the magnetic properties of our NC films.

To correlate the differences between the magnetic behavior of the films with the atomic structure, we performed XAS and XMCD at beamline 4.0.2 of the Advanced Light Source to obtain element and valence specific information. The Fe XAS spectra (Figure 3(a)) for all films have the same characteristic features. The small peak around 707-eV on the lower-energy shoulder of the L_3 edge is indicative of higher concentrations of Fe^{3+} or lower concentrations of Fe^{2+} . In Figure 3(b), the L_3 XMCD spectra for Fe are shown, normalized by the XMCD peak at 708.6 eV, which corresponds to Fe^{3+} with octahedral coordination.¹³ The two lower-energy peaks convey information on the relative concentrations of Fe^{2+} compared to Fe^{3+} in octahedral and tetrahedral sites, respectively, as indicated in Figure 3(b).^{13,14} It is clear that there is a greater concentration of Fe^{3+} with tetrahedral coordination in NC films relative to the epitaxial films. The NC films also have higher concentrations of Fe^{2+} relative to Fe^{3+} in the octahedral sites, as compared to epitaxial films. The existence of mixed 2+ and 3+ cations in the octahedral sites is thought to be beneficial for inducing an intervalence charge transfer under incident optical signals. Such a cation distribution may enhance the photomagnetic properties of complex oxides, particularly for manganese zinc ferrites and related compounds.^{15,16} Furthermore, the existence of both Fe^{3+} in the tetrahedral sites and Fe^{2+} in the octahedral sites could result in a lower moment, though the main reason for the suppressed moment likely stems from magnetic frustration arising from microstructural disorder in the NC films. The increase in the mixed nature of Fe^{3+} occupancy in the NC films suggests that variations in cation occupancy could potentially be used to design materials with alternative charge transfers and a photomagnetic effect induced by an electronic transition.

In summary, we have demonstrated a straightforward way to achieve NC spinel ferrite films with varying degrees of crystallinity without exposing samples to conditions above room temperature. While epitaxial thin films of MZFO are highly crystalline and exhibit symmetric hysteresis loops with high saturation magnetization values, the films deposited at room temperature show exchange biasing at low temperatures and exhibit reduced magnetization values even at high fields. The magnetic properties of these NC MZFO thin films can be explained by the coexistence of crystalline regions surrounded by more disordered regions. The exchange bias is attributed to coupling between the ferrimagnetic and magnetically frustrated regions. Together these results indicate that controlling the presence of MZFO nanocrystallites that are weakly coupled to each other is an effective means of tuning the magnetism.

We thank Gopalan Srinivasan for the MZFO targets and K. M. Yu for his assistance in RBS data collection. We also thank Jostein Grepstad, Chunyong He, John L.R. Watts, Matthew Gray, Ted Sanders, Kari Thorkelsson, Jayakanth Ravichandran, Morgan Trassin, and Matt Lucas for useful discussions. This work was supported by the Office of Naval Research under Grant No. N00014-10-1-0226. U.S.A. is supported by a National Science Foundation Graduate Research Fellowship. F.J.W. is supported by the Army Research Office under Grant No. MURI W911NF-08-1-0317. A.J.G., V.V.M., and the Advanced Light Source are supported by the Director, Office of Science, Office of Basic Energy Sciences, of the U.S. Department of Energy under Contract No. DE-AC02-05CH11231. J.M.I. is supported by the NSF Grant Nos. 0604277 and 1104401.

¹Y. Suzuki, *Annu. Rev. Mater. Res.* **31**, 265 (2001).

²T. Holtwijk *et al.*, *IEEE Trans. Magn.* **MAG-6**, 853 (1970).

³K. Hisatake *et al.*, *Jpn. J. Appl. Phys.* **15**, 1823 (1976).

⁴H. D. Jonker, *J. Solid State Chem.* **10**, 116 (1974).

⁵E. Katsnelson, *J. Appl. Phys.* **69**, 4556 (1991).

⁶W. Lems *et al.*, *Phys. Rev. Lett.* **21**, 1643 (1968).

⁷E. Katsnelson, *J. Appl. Phys.* **77**, 4604 (1995).

⁸J. S. Bettinger *et al.*, *Appl. Phys. Lett.* **94**, 072505 (2009).

⁹A. L. Patterson, *Phys. Rev.* **56**, 978 (1939).

¹⁰B. D. Cullity, *Elements of X-Ray Diffraction* (Prentice-Hall, Upper Saddle River, NJ, 2001), p. 400.

¹¹J. Nogués *et al.*, *Phys. Rep.* **422**, 65 (2005).

¹²S. Venzke *et al.*, *J. Mater. Res.* **11**, 1187 (1996).

¹³N. D. Telling *et al.*, *Appl. Phys. Lett.* **95**, 163701 (2009).

¹⁴J.-S. Kang *et al.*, *Phys. Rev. B* **77**, 035121 (2008).

¹⁵J. S. Bettinger *et al.*, *Phys. Rev. B* **80**, 140413(R) (2009).

¹⁶R. W. Teale and D. W. Temple, *Phys. Rev. Lett.* **19**, 904 (1967).